Surface & Coatings Technology 311 (2017) 127–137

Contents lists available at ScienceDirect

Surface & Coatings Technology

journal homepage: www.elsevier.com/locate/surfcoat

Effect of the plasma excitation power on the properties of $SiO_xC_yH_z$ films deposited on AISI 304 steel

Nazir M. Santos [a], Thais M. Gonçalves [a], Jayr de Amorim [b], Celia M.A. Freire [c], José R.R. Bortoleto [a], Steven F. Durrant [a,*], Rafael Parra Ribeiro [a], Nilson C. Cruz [a], Elidiane C. Rangel [a]

[a] Laboratory of Technological Plasmas, UNESP, Sorocaba, SP, Brazil
[b] Brazilian Bioethanol Science and Technology Laboratory, CTBE, Campinas, SP, Brazil
[c] Department of Materials Engineering, UNICAMP, Campinas, SP, Brazil

ARTICLE INFO

Article history:
Received 29 August 2016
Revised 26 November 2016
Accepted in revised form 29 December 2016
Available online 30 December 2016

Keywords:
HMDSO
Chemical composition
Barrier properties
Corrosion resistance
Polymers films
PECVD

ABSTRACT

Films were produced on stainless-steel substrates by radiofrequency Plasma Enhanced Chemical Vapor Deposition (RF-PECVD) of mixtures containing 70% hexamethyldisiloxane, 20% oxygen and 10% argon. While the plasma excitation power was varied from 15 to 75 W, the deposition time and total gas pressure were kept constant at 1800 s and 8.0 Pa, respectively. The influences of the plasma power on the plasma kinetics and the ion bombardment of the growing film are discussed. Film composition and chemical structure were determined using X-ray photoelectron- and infrared reflectance-absorbance spectroscopy, respectively. Profilometry was used to measure the thicknesses of the resulting layers. The root mean square roughness was evaluated from surface topographic profiles acquired by atomic force microscopy. Scanning electron microscopy and energy dispersive spectroscopy were employed to evaluate the morphology and elemental composition of the coatings. Electrochemical impedance spectroscopy and potentiodynamic polarization tests were used to derive the corrosion resistance of the samples to a saline solution. Substantial changes in the material structure and progressive increases in film thickness were observed with increasing applied power. The resulting material was an organosilicon layer composed of Si—O backbones surrounded by methyl groups, very similar to conventional polydimethylsiloxane. Increases in the proportions of Si—O and methylsilyl groups in the structure were observed at greater plasma excitation powers, indicating densification of the structure owing to greater ion bombardment. The surface morphology and roughness were also dependent on the treatment power. Independently of the deposition conditions, application of the film increased the corrosion resistance of the stainless steel. A 10,000-fold elevation in the total system resistance under electrochemical testing was achieved for the film prepared with the greatest ion bombardment intensity. Film thickness was observed to be a key parameter but the coating structure had a major effect on this result.

© 2016 Elsevier B.V. All rights reserved.

1. Introduction

Plasma Enhanced Chemical Vapor Deposition, PECVD, has emerged as a clean, simple and cost-effective methodology for the production of silicon-based coatings. Many studies, employing plasma deposition and hexamethyldisiloxane, HMDSO, as the starting material, have demonstrated the convenience of this method to prepare nanocomposites for the controlled release of silver [1], ice repellent coatings [2], humidity sensors [3], gas permeation barriers [4], dielectric films for gates in MgZnO transistors [5], corrosion resistant layers for Al 2024 and magnesium [6–7] as well as protective gradient coatings [8]. Thus, a broad range of structures have been prepared using the PECVD of HMDSO.

More specifically, many studies [9–11] have been devoted to the development of alternative techniques for reducing or preventing the corrosion process of metallic surfaces. Amongst the extant plasma deposition studies, however, most are focused on the protection of iron [12,13], magnesium [14], bell metal [15] and aluminum [16,17], materials which present lower corrosion resistance than stainless steel.

Silica films are frequently adopted as barriers for metal corrosion protection since they are more inert and denser than the silicone-like coatings. However, SiO_x-like films, also present drawbacks related to surface defects, adherence, porosity, intrinsic stress, and rigidity which hinder further improvements in the barrier properties and, consequently, in the corrosion protection. Despite their lower inertness and density, organosilicon films present smoother, more flexible networks, which exhibit good adhesion to diverse substrates. Some of the disadvantages of using the organosilicon structure could be overcome if its degree of crosslinking could be increased. Reticulation, which connects neighboring

* Corresponding author at: Laboratório de Plasmas Tecnologicos Instituto de Ciência e Tecnologia de Sorocaba UNESP 18087-180 Sorocaba, SP Brazil.
E-mail address: steve@sorocaba.unesp.br (S.F. Durrant).

http://dx.doi.org/10.1016/j.surfcoat.2016.12.113
0257-8972/© 2016 Elsevier B.V. All rights reserved.

chains, tends to approximate the silicon backbones, and therefore, to decrease the interatomic spacing, thereby increasing the film density. The physical stability, inertness, and permeability are affected by this process, thus improving barrier properties [7].

According to Fanelli et al. [18], electron collision plays the major hole in the fragmentation of HMDSO, even if high proportions of oxygen are present in the plasma. Indeed, siloxane films prepared from HMDSO plasmas are generally deposited using high oxygen additions [18–21]. The findings show that either greater applied powers [22] or greater proportions of oxygen [18] produce a transition from an organic to an inorganic SiO_x-like material. Although this structural change is beneficial regarding density, when high oxygen proportions are used the proportion of silanol groups increases. Silanol groups act as degradation initiator points and, therefore, reduce the inertness of the coating. Adhesion of the film to the substrate also affects its anti-corrosion performance. Owing to improved adhesion despite its lower density [20], a uniformly adhered organosilicon layer, prepared in plasma fed HMDSO presents better anti-corrosive protection than its SiO-like counterpart.

The objectives of this study are as follows: (i) to investigate whether the degree of crosslinking and silanol content of HMDSO-derived films can be tailored by the plasma excitation power while maintaining the convenient organosilicon structure; (ii) to evaluate whether there is any correlation amongst the structural changes and the corrosion protection provided to stainless steel. For this, excitation power was chosen as the key process parameter since it promptly affects the density or the energy distribution of the plasma species or both and may not increase the silanol content. Low oxygen dilution was employed for the same reason. Radiofrequency power was supplied to the sample holder to promote low energy ion bombardment of the growing layer in an attempt to promote cross-linking between chains [23]. Therefore, the novelty of the work consists in investigating whether the degree of crosslinking can be controlled in the organosilicon structure and how it affects the saline corrosion resistance of stainless steel, an already highly inert material.

2. Experimental

The plasma cleaning, treatment and deposition processes were conducted in a capacitively coupled plasma reactor. A complete description of the system is found elsewhere [24], but essentially, it is composed of a stainless-steel reactor, a vacuum system and an electrical power generator. The reactor contains two horizontal parallel-plate stainless steel electrodes, capacitively coupled to a 13.56 MHz power supply through a matching network. Gases are admitted to the reactor through plastic tubes via needles valves. The system pressure is monitored by a capacitance gauge and controlled by needle valves. To generate plasma in this configuration, the lower electrode is fed RF power; the upper electrode is earthed.

In this work, films were deposited on plates of AISI 304 stainless steel, of polished silicon and of glass. The substrates were chemically cleaned in ultrasonic baths [25], dried in a hot air flow, and then placed on the lowermost electrode of the plasma reactor. To eliminate the native oxide layer, prior to each deposition, the substrates were further cleaned in an argon plasma (70 W, 15 Pa, 600 s). The samples were subsequently treated in oxygen plasmas (50 W, 10 Pa, 300 s), to grow a new oxide layer under controlled conditions, as reported by Fracassi [26]. Films were then deposited for 1800 s in plasmas generated from 70% HMDSO, 20% oxygen and 10% argon at a total pressure of 8.0 Pa. While the precursor flow, pressure and deposition time were fixed for all the experiments, excitation power, P, was increased from 15 to 75 W. The effect of this parameter on the properties of the films was investigated.

A homemade low-pass filter was used to measure the induced self-bias voltage on the powered electrode. Composed of inductors and capacitors, the filter was tuned to block the 13.56 MHz RF power, allowing only the DC (direct current) induced voltage to be measured by a voltmeter connected in parallel with the electrodes.

The thickness of the films was measured using a Veeco Dektak 150 profilometer, from a film step-height produced by partially masking the glass substrate with a Kapton tape prior to deposition and removing it afterwards.

The morphology of the samples was inspected by Scanning Electron Microscopy, SEM, using a Jasco JSM6010 instrument. Secondary electron (SE) micrographs were generated of the surface of films deposited onto stainless-steel and silicon substrates and from cross-sections of those prepared on silicon. Beam energies of 3 and 10 keV were used. Prior to the SEM imaging, a thin conductive layer was deposited onto the surfaces by plasma sputtering (40 mA, 60 s) of an Au-Pd alloy. The surface roughness of the as-received and plasma-treated stainless steel was calculated from scanning probe Atomic Force Microscopy (AFM) images, acquired in the contact mode using a Park System XE 100 microscope. The area of each scan was 20×20 μm^2.

Film chemical structure was investigated using Infrared Reflectance Absorbance Spectroscopy (IRRAS) (Jasco FTIR, model 410) of samples prepared on polished AISI 304 steel. Transmission spectra, within the range from 4000 to 400 cm^{-1}, were obtained by collecting 128 scans for each sample at 4 cm^{-1} resolution. The surface chemical composition was examined using a SPECSLAB II (Phoibos-Hs 3500 150 analyzer, SPECS, 9 channels) X-ray Photoelectron Spectrometer, which employs a non-monochromatic Al K_α ($h\nu = 1486.6$ eV) X-ray source. The carbon line at 284.4 eV was used as a reference to determine the binding energy (BE) of O 1s, C 1s and Si 2p core electrons. These calculations were performed using the Casa XPS software (version 2.3.13). The accuracy of the BE values was ± 0.1 eV. Elemental composition was also determined by energy dispersive spectroscopy, EDS, using an X-ray (Dry SD Hyper) detector coupled to the scanning electron microscope (Jasco JSM6010). Energy resolution was of 129–133 eV for the Mn K-α line at 3000 cps.

Electrochemical Impedance Spectroscopy (EIS) and potentiodynamic polarization tests were used to investigate the corrosion resistance of the as-received and plasma-treated AISI 304 steel. EIS measurements were carried out at the open circuit potential, applying a sigmoid function (10 mV) in the frequency range 10^{-2}–10^5 Hz. A potentiostat PAR 273A-EG&G, with POWERSINE-PAR software for data acquisition, was used in these experiments. A three-electrode electrochemical cell was employed: a Saturated Calomel Electrode (SCE) as reference, a platinum foil as counter electrode, the plasma-treated AISI 304 steel as the working electrode. Potentiodynamic polarization was used to evaluate the resistance to corrosion pitting of as-received AISI 304 steel and steel coated with plasma-deposited film. The potentiodynamic polarization curves were taken in relation to the open circuit potential (OCP), by applying a potential scan from -1.0 V to $+1.5$ V, at a rate of 1 mVs^{-1}. An Autolab PGSTAT 128N with Nova 2.1 software was used for the data acquisition. An electrochemical cell with three electrodes was employed: a Ag/AgCl/3M KCl ($+210$ mV vs SHE) electrode was used as a reference, a stainless-steel disk as a counter electrode and AISI 304 steel as-received and covered with plasma-deposited film, having an exposed area of 1 cm^2, as the working electrode. The measurements were realized after an immersion time of 1800 s. Electrochemical measurements were performed at the center of the samples using 3.5% NaCl solution (pH 6.2).

3. Results and discussions

Fig. 1 shows the thickness of the films as a function of P. Films with thicknesses ranging from 400 to 2150 nm were obtained by increasing the plasma excitation power from 15 to 75 W. As the deposition time was kept constant (30 min) the deposition rate followed the same trend as the film thickness, increasing from 17 to 67 nm min^{-1}.

For films deposited under conditions very similar to those employed here [15] slightly lower (14.4 to 28.5 nm min^{-1}) deposition rates were found in the 20 to 70 W power range, with the differences being

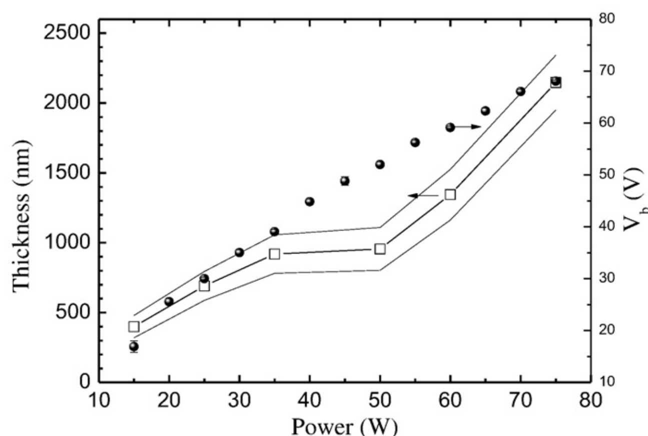

Fig. 1. Thickness of the films and self-bias voltage as a function of the plasma excitation power for the depositions undertaken. The flow of feed components, deposition time and pressure were kept constant for all the experiments.

attributed to the different working pressures. On the other hand, greater deposition rates (40 to 140 nm min^{-1}) were obtained in the work of Vautrin-Ul et al. [13], using a microwave excited plasma (80% of HMDSO and 20% of O_2) while biasing the sample holder with radiofrequency power (0 to 120 W). A rise in self bias polarization enhanced the deposition rate. Another result very similar to those presented here is found in the work of Zhou et al. [27], who used HMDSO/Ar/O_2 dielectric barrier discharges but no self-bias voltage.

The rising trends in thickness and deposition rate can be attributed to the effect of P on the average energy and density of the electrons in the plasma [22], affecting the overall plasma activation rate. Aside from this, is the influence of P on the ion bombardment mechanism. Studies in the literature propose that the self-bias voltage of the driven electrode, V_b, depends on the radiofrequency excitation power. To evaluate this relationship, V_b was measured; the results are depicted in Fig. 1. A progressive increase in V_b from 15 to 70 V was seen as the excitation power was enhanced from 15 to 75 W, in good agreement with results of a previous investigation [28]. Therefore, the rise in V_b with increasing P, at constant pressure, affects the probability of ionized fragments reaching the substrate surface, which is a factor that may change the deposition rate.

Experimental data (not shown) demonstrated that increasing the power beyond 75 W resulted in detachment of the films from the substrates, suggesting an increase in the intrinsic stress with increasing film thickness. Despite this observation, films with high thickness (1–2 μm) and good physical stability were obtained using excitation powers of up to 75 W. The good stability of the coatings, even after aging in air, is in part due to the improved adhesion promoted by plasma cleaning and treatment of the stainless steel native oxide conducted before the deposition procedure.

Fig. 2(a) shows infrared spectra of the films in the 4000 to 400 cm^{-1}-range; Fig. 2(b) shows infrared spectra in the 1200 to 400 cm^{-1} range. The wavenumbers of the main absorptions and their respective assignments are summarized in Table 1. A broad band between 3750 and 3200 cm^{-1}, which is attributed to O—H stretching in silanol groups (Si—OH), is observed in the spectra.

One of the most prominent peaks, lying between 1000 and 1200 cm^{-1}, is a doublet composed of the symmetrical (1100 cm^{-1}) and asymmetrical (1020 cm^{-1}) stretching modes of Si—O in Si—O—Si groups [29]. Organic groups are shown to be present by the bands centered at 2900 (sym. ν C—H), 2960 (asym. ν C—H), 1400 (δ C—H) 1260 (ν C—H in ($Si(CH_3)_x$)), 840 (δ C—H in ($Si(CH_3)_3$)) and 780 cm^{-1} (δ C—H in ($Si(CH_3)_2$)). The latter three absorptions reveal the retention of the HMDSO structure in the plasma deposit. The presence of the dimethylsilyl group ($(SiCH_3)_2$), a chain propagation unit, suggests the formation of a structure similar to that of conventional PDMS

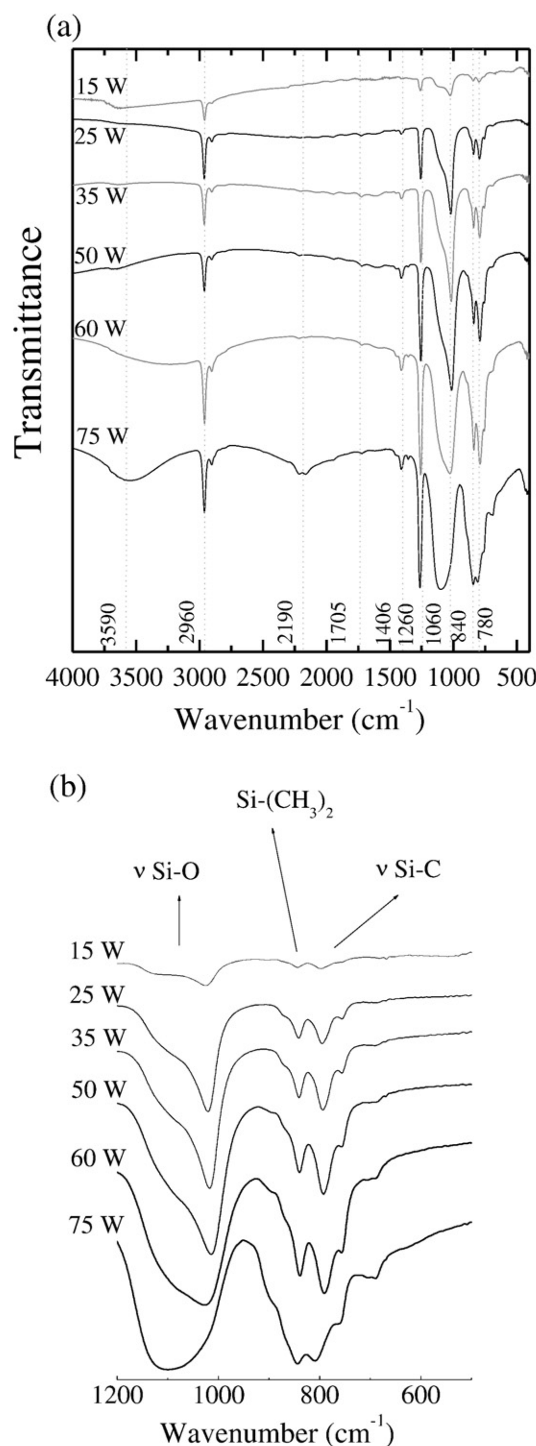

Fig. 2. Transmission infrared spectra of pp-HMDSO films deposited at different powers (a) 400–4000 cm^{-1} and (b) 1200–400 cm^{-1}.

(polydimethylsiloxane) which is terminated with $Si(CH_3)_3$ functionalities [18]. The schematic representation of such a structure is given in Fig. 3.

Carbonyl groups (C=O), detected by the weak band around 1700 cm^{-1}, originate from oxidative reactions in the plasma phase or by plasma-surface interactions due to oxygen present in the gas mixture [22]. For films deposited at powers ≥50 W, a peak around 2190 cm^{-1}, characteristic of the Si—H stretching vibration, also emerges. Generally, Si—H is detected as a lateral or termination group in high molecular weight fragments (higher than that of HMDSO) [18], indicating further

Table 1
Wavenumber and assignments of the bands detected in the infrared spectra of the films.

Wavenumber (cm^{-1})	Assignments	Groups
3750–3200	—OH stretching mode	Si—OH
2900–2960	CH_x symmetric and asymmetric stretching	CH_3 and CH_2
2190	SiH stretching mode	SiH
1705	C=O stretching mode	CH_2O
1406	C—H_3 symmetric bending	$Si(CH_3)_x$
1260	CH_3 symmetrical bending mode	Si-$(CH_3)_x$
1200–1000	Si—O asymmetrical stretching mode	Si-O-Si
840	CH_3 rocking	Si-$(CH_3)_3$
780	CH_3 rocking	Si-$(CH_3)_2$

differences between the conventional PDMS and the silicone-like plasma deposited material. The intensity of this band thus indicates the degree of fragmentation of trimethyl-silyl groups [30]. As indicated by points 1, 2 and 3 of Fig. 3, this fragmentation constitutes part of the main propagation route for film ramification [18].

The good adhesion of the film to the substrate is ascribed to the existence of covalent bonds between O of the film (Si—O) and the treated metallic oxide structure (Fig. 3). Furthermore, the extra energy provided by ion bombardment counter-balances the rise in the internal stress induced by the increase in deposition rate/film thickness, thus explaining the stability of the films investigated here despite their relatively high thicknesses.

Comparing the spectra of Fig. 2(b) reveals an increase in the overall intensity of the bands, which correlates well with the film thickness (Fig. 1). But thickness changes are not the only reason for the evolution observed in the spectra of Fig. 2(b). Structural changes also take place. Support for this inference is obtained by analyzing the behavior of the Si—O band (~1000 cm^{-1}). For the low P regime (≤50 W) the component attributed to the asymmetric mode (1020 cm^{-1}) is more prominent, while for high P levels (>50 W), the contribution associated with the symmetric (1100 cm^{-1}) vibrations rises, reaching practically the same intensity as that of the asymmetric one. Also interesting is the shift of this band to greater wavenumbers as the deposition power is increased from 60 to 75 W. This evolution can be attributed to the increase in the proportion of Si—H, which inhibits cross-linking between chains and thus tends to decrease the film density [13].

Another example of structural alteration is related to the continuous broadening of the Si—O band. This effect is explained in terms of the addition of different species to the Si—O—Si environment, generating contributions at a variety of wavelengths, which overlap into a single envelope. For the same reason, the peaks observed around 840-(Si-$(CH_3)_3$) and 780 cm^{-1} (Si-$(CH_3)_2$) merge into each other in the spectra obtained from the films deposited at higher applied powers. Such band broadening is consistent with an increase in plasma fragmentation at higher applied power and with the increasing energy transferred to the growing layer by ionic impacts. The latter process contributes to the production of new reactive sites on the growing polymer surface, which can also account for the addition of different groups to the polymeric backbone.

In the work of Fanelli et al. [18] it is postulated that the primary fragmentation of the HMDSO molecule occurs preferentially at the Si—O bond by electron impact, despite its high energy compared to the Si—C of the methylsilyl groups. Through oligomerization reactions, longer chains are then formed, generating molecules with molecular weights greater than that of HMDSO [22]. The relative increase in the intensity of the peak at 780 cm^{-1} with respect to the C—H band intensity (2980 cm^{-1}), attributed to ($Si(CH_3)_2$), which represents propagation units in the chain (vertical backbone in Fig. 3), suggests the formation of longer silicon backbones at greater plasma powers [31]. Furthermore,

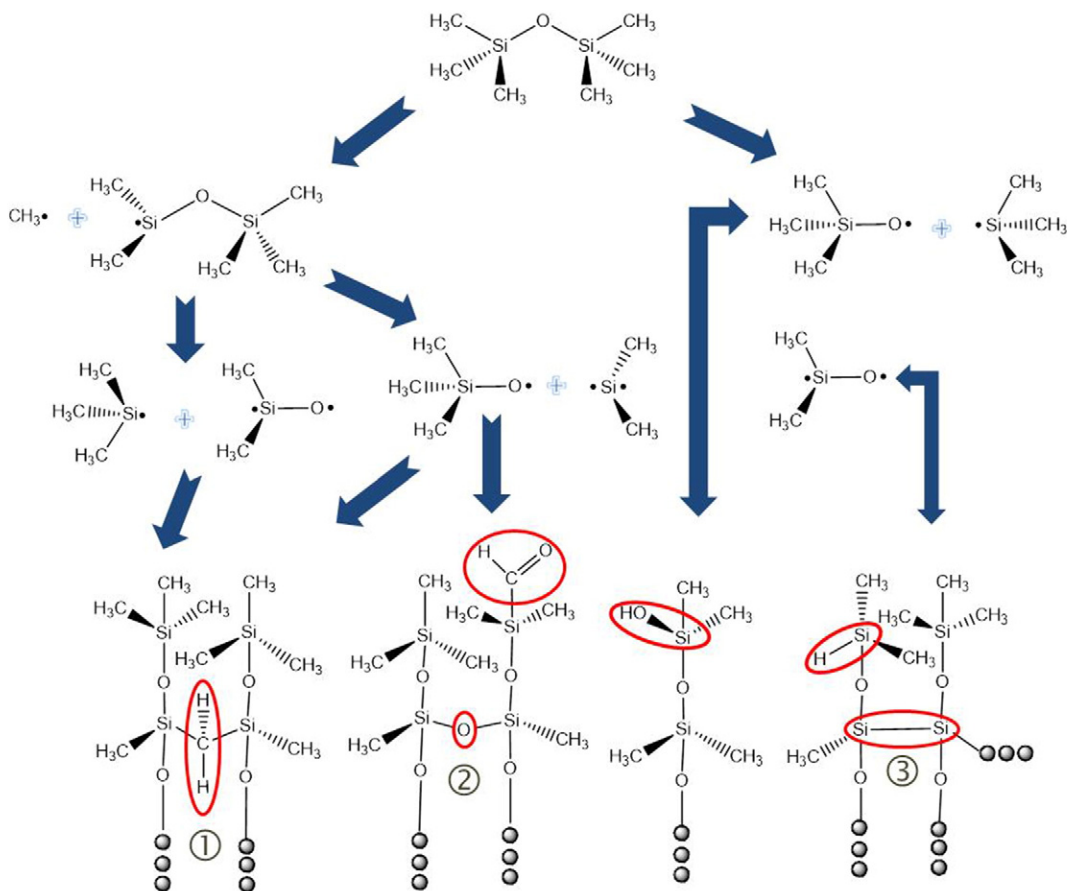

Fig. 3. Schematic representation of the structure formed by plasma polymerization of HMDSO.

the scission of C—H bonds in Si-CH_3 groups in the plasma or by plasma-surface interactions, effectively accounts for crosslinking (horizontal backbone in Fig. 3) and the incorporation of a series of functional groups in the film structure as reported by Blanchard and co-workers [31].

To further evaluate the effect of the plasma excitation power on the chemical structure of the films, the relative density of Si—O groups, [SiO], was evaluated from areas of the band at 1100 cm^{-1}, using the model proposed by Lanford and Rand [32]. The results are depicted in Fig. 4(a) as a function of P. The overall tendency is towards greater relative densities for the range of powers between 25 and 60 W. An increase in the Si—O density with increasing self-bias was also encountered in the work of Zajíčková et al. [23] and Vautrin et al. [13] in experimental conditions similar to those used here.

The relative densities of CH_x (2960 cm^{-1}), OH (3750–3200 cm^{-1}), $Si(CH_3)_x$ (1260 cm^{-1}) and SiH (2190 cm^{-1}) were also evaluated and are presented in Fig. 4(b) as a function of P. Although the absolute values cannot be compared between species, the tendencies in the density of each species as a function of P are revealed. A general decrease can be seen in the curve which represents the relative density of CH_x species, [CH_x], as P is increased from 25 to 75 W. On the other hand, the relative density of methyl groups in $Si(CH_3)_x$, [$Si(CH_3)_x$], increases for depositions performed with P ranging from 25 to 60 W. Indeed, the trends in [$Si(CH_3)_x$] and [SiO] are exactly the same, indicating that power is not affecting the organosilicon nature of the structure but rather the deposition rate and degree of compaction.

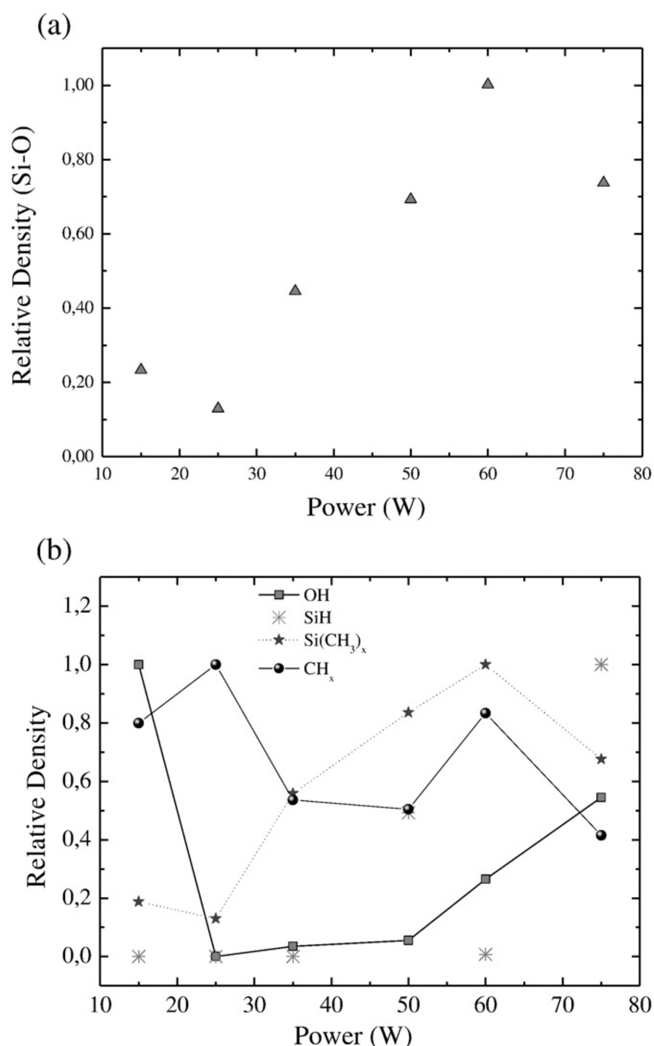

Fig. 4. Relative density of SiO (a) and of OH, CH_x, $Si(CH_3)_x$ and SiH (b) in the film as a function of the plasma excitation power.

In the low P regime, the lower average energy of the plasma electrons is consistent with a lower concentration of precursor fragments and thus with reduced deposition rates. It is postulated that only slight variations in the plasma kinetics occur, contributing to fragmentation of trimethylsilyl groups. But in general, the system is operating in the lack-of-energy regime since the nature of the incorporated fragments is not significantly changed by further increasing P. Only the deposition rate is severely affected under such conditions.

The relative density of —OH groups, [OH], initially falls but then increases for P > 25 W. Hydroxyl groups could originate from multiple-step reactions in the plasma phase since oxygen was incorporated into the gas mixture and is present in the HMDSO molecule itself. Heterogeneous gas-solid reaction may also account for incorporation of oxidized (OH, C=O) species especially if ion bombardment is present. The deposition of energy by ion bombardment promotes emission of lateral and terminal groups of the chains, such as CH_X and H. This phenomenon contributes to the creation of unstable pendant bonds which tend to be absorbed by chain crosslinking. But this absorption only occurs when the density of radicals is sufficient to enable recombination. The distance between radicals is another relevant issue. If crosslinking is not possible, radicals are left active in the structure and tend to incorporate oxidized groups from the atmosphere when the sample is withdrawn from the vacuum chamber.

The initial fall in [OH] and its constancy at near null values afterwards are indicative of an increase in the degree of cross-linking. As illustrated in Fig. 3 (adapted from Blanchard and co-workers [31]), the connection of neighboring chains through covalent bonds produces a structure similar to, but more crosslinked than, conventional silicone. The final increase in [OH] and [Si—H], simultaneously with the fall in [SiO] and [$Si(CH_3)_x$], indicates structural rarefication upon an increase in the ion bombardment and also in the deposition rate. According to Fracassi [26], the variation in the proportion —OH density of pp-HMDSO films may be related to modifications in the degree of cross-linking.

In summary, considering the conditions employed here, the excitation power apparently has no further effect on the plasma kinetics than increasing the deposition rate. The major effect on the molecular structure of the films is produced by heterogeneous reactions induced by ion bombardment.

Atomic concentrations of carbon, [C], silicon, [Si], and oxygen, [O], in the films, calculated from the XPS spectral data, are depicted in Fig. 5(a) as a function of the plasma excitation power. If the hydrogen content, which cannot be measured by XPS, is ignored, the films are composed of about 47% carbon, 30% silicon and 23% oxygen. These proportions are roughly the same as those encountered in the work of Alexander et al. [22] and match well with the composition of conventional polydimethylsiloxane, that is, 50% C, 25% Si and 25% O. Comparing the measured and expected atomic proportions, an enrichment of Si and a reduction in C is seen, consistently with the loss of lateral groups from the structure together with an increase in crosslinking (as schematized in Fig. 3).

Once again neglecting the H content, and considering the HMDSO molecule, [C], [Si] and [O] are in the proportions 67%, 23% and 10%, respectively. That is, the formation of a deposit from HMDSO occurs via molecular fragmentation, which involves a substantial loss of C and very possibly of H. Thus, relatively high proportions of Si and especially of O in the solid phase are ascribed to the fragmentation of the organosilicon molecule in the plasma environment, producing light neutral species such as C_2H_2, CH_4, C_2H_6, and C_3H_8. The non-reactive nature of such fragments reduces the probability of their incorporation into the film structure [22,23]. Oxidation of the organic fragments, producing groups with low sticking coefficients, also contributes to reduction of C in the solid phase. The relatively high proportion of Si remaining in the film also indicates considerable cross-linking [22,23].

The high resolution Si 2p spectra of the samples were fitted using four components centered at 101.5 eV ($SiO(CH_3)_3$), 102.1 eV

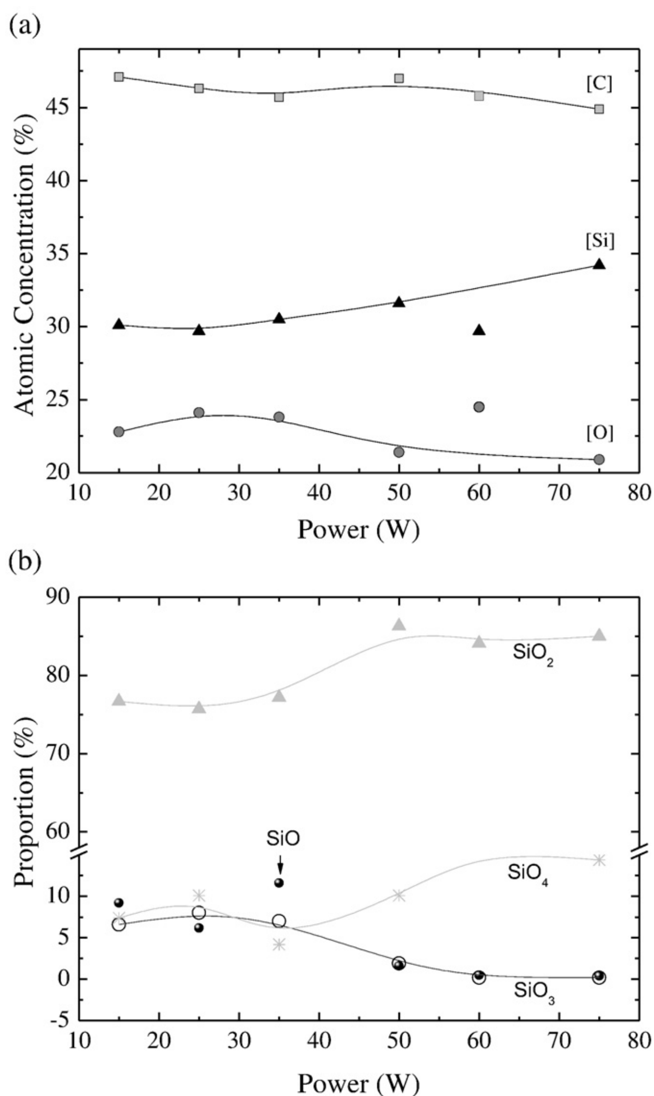

Fig. 5. (a) Atomic concentration of carbon, silicon and oxygen in the films as a function of the plasma excitation power. (b) Relative proportion of each type of silicon bond contributing to the Si 2p peak as a function of the plasma potential.

($SiO_2(CH_3)_2$), 102.8 eV ($SiO_3(CH_3)$) and 103.4 eV (SiO_4) consistently with previous works [33–35]. The proportion of each contribution to the total area of the peak was evaluated and is depicted in Fig. 5(b) as a function of P. Independently of the deposition condition, SiO_2(dimethylsiloxane) is the predominant group in good accordance with the PDMS-like structure derived from the infrared spectroscopy results. The proportion of this group further increases for P > 35 W while those related to SiO (trimethylsiloxane) and SiO_3 (methylsiloxane) groups are reduced, vanishing at the highest powers. Further evidence for methyl abstraction is provided by the increase in the proportion of SiO_4.

Despite the changes observed in the molecular structure of the films at greater plasma powers, chemical composition is barely affected. Similar results were observed previously [36]. In the power range used here the organosilicon nature of the film was preserved together with promotion of inter-chain connections due to ion bombardment. The ratio between the fluxes of charged to neutral species reaching the substrate seems to dominate the structure densification/rarefication process. As the deposition rate increases rapidly, the energy deposited by ionic impact is diluted and crosslinking is not effective. The balance between deposition rate and ion bombardment, which most favors crosslinking, was observed at 60 W.

Fig. 6 shows $20 \times 20\ \mu m^2$ topographical images of the bare stainless steel and of the coated samples. On the surface of the bare steel the grain boundaries of the alloy, and the chemical polishing marks, characterized by dark, parallel, horizontal lines, are readily observed. Some scratches, possibly generated by the polishing process, can also be seen. Furthermore, the distinct textures noticed in the image are associated with distinct phases in this material.

The morphology of the substrate is largely retained even after plasma deposition, indicating that the film follows the topography of the steel. At low plasma power (25 W) the deposition results in uniform films containing sparsely scattered particles, whose concentration grows with increasing power, thus promoting the transition from a uniform to a granular structure. For the sample prepared at the greatest power an organized pattern of the particles, defined by the texture of the grains in which they were deposited, is clearly observed. Owing to the increase in the coating thickness the substrate grain boundaries become less distinct in this sample. Wang et al. [37] also observed the dependency of the film morphology on the type of substrate - glass, polypropylene or polyethylene. No film detachment was detected throughout the inspected areas of each sample.

The granular structure of the films prepared from HMDSO-containing plasmas is related to the plasma-phase polymerization stimulated by oxygen present in the mixture [38]. Particulates of different molecular weight are formed in the plasma phase and are incorporated into the film structure due to electrostatic or gravitational forces. The rate at which the particles are formed depends on the proportion of oxygen in the plasma and on the plasma excitation power since these parameters affect the availability of reactive precursors in the plasma. Argon is known to reduce polymerization in the plasma phase and hence the concentration of particulates incorporated into the film.

The intensity of ionic bombardment is also relevant. Vautrin et al. [13] demonstrated the influence of the self-bias polarization on the morphology of films deposited from HMDSO/O_2 plasmas. A substantial decrease in the particle grain size with increasing RF bias was seen to result from a greater number of reactive sites created on the surface by ionic bombardment. In the present work, the concentration and diameter of particles is observed to increase with increasing V_b. This morphological evolution is attributed to a balance between the effect of the applied power on the availability and size of agglomerates in the plasma phase and that of the greater ionic bombardment experienced at greater applied powers.

Fig. 7(a) shows cross-sectional micrographs of the films deposited on Si substrates using three different deposition conditions. The plasma deposited film is readily detected in the micrographs by visual inspection as well as by its compositional characteristics. As inclination was not controlled in these experiments, the thickness of the layer could not be directly determined from the micrographs. A uniform interface along the entire extension of the Si surface is, however, clearly visible. The integrity of the film-substrate interface even after cleavage indicates the good physical stability and adhesion of the coatings. The top-view micrographs of the samples prepared on Si and stainless steel substrates are presented in Fig. 7(b) and (c) respectively, showing the same surface morphology despite the different substrates.

The mean square roughness, RMS, of the samples, determined from the images presented in Fig. 6, is depicted in Fig. 8 as a function of P. For the bare steel the RMS value is represented by the dotted line. With the exception of the film prepared at 15 W, which presented the most regular surface, film deposition increases roughness. Two gradients are observed in the curve, the first as power increases from 15 to 25 W and the second, as P increases from 50 to 60 W. Both trends are ascribed to an increase in the proportion of particulates in the structure.

The corrosion resistance of the samples to saline solution was evaluated by electrochemical impedance spectroscopy and potentiodynamic polarization tests, using samples prepared on stainless steel at different plasma excitation powers and then with different thicknesses. Fig. 9(a) shows the results for the impedance modulus, |Z|, as a function of

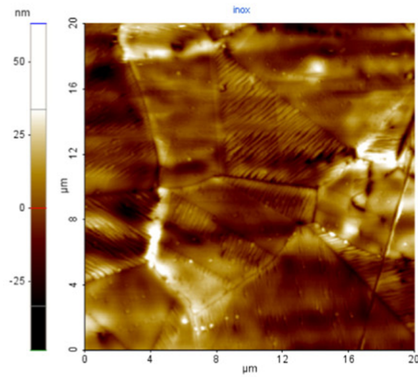

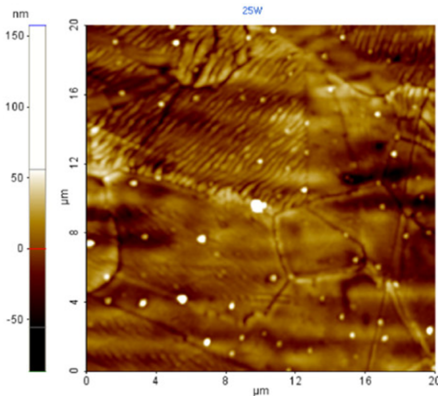

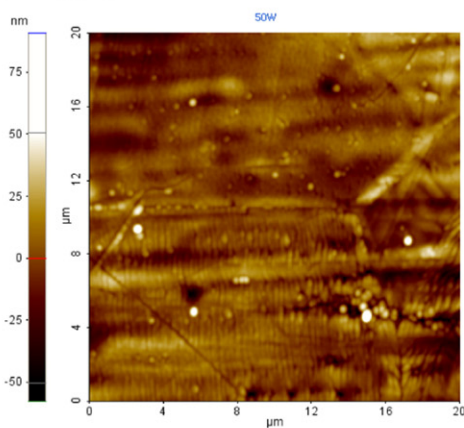

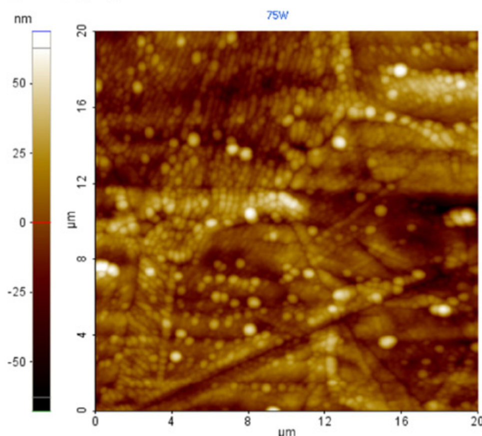

Fig. 6. 20 × 20 μm^2 atomic force microscopy image of the bare stainless steel and of the steel treated at different applied powers.

frequency. Results for the as-received stainless steel are also presented. At greater powers the curves are shifted upwards, which is consistent with a better performance in the corrosive environment. While all the films protected the steel, the best results were found for films prepared at the greatest excitation powers (60 and 75 W).

Fig. 9(b) presents the phase angle, which defines the difference in phase between voltage and current, as a function of frequency for the different samples. For the bare steel, a curve with one concavity is obtained with a maximum around 10^0 Hz. Upon film deposition the behavior of the phase angle with frequency is substantially altered. First, at the high frequency edge (10^5 Hz), the curves begin with greater phase angles (60 to 90°) than that of the bare steel (<10°), indicating the presence of the protective film. For the system prepared with 15 W, the phase angle falls in the low frequency region, generating a second concavity centered around 10^{-1} Hz. The same behavior is observed for the phase angle of the systems deposited at 35, 50 and 75 W, with the second concavities arising at around 10^1, 10^0 and 10^{-1} Hz, respectively. For the samples containing the films deposited at 25 and 60 W, the frequency variation hardly affects the phase angle. Consistently, an overall elevation in the corrosion (E_{corr}) and pitting (E_{pit}) potential was observed for the sample treated in 25 W plasmas while the rise was substantially lower (20%) for those exposed to treatments of 50 and 75 W, as derived from the potentiodynamic polarization results depicted in Fig. 10(a) and in Table 2.

The absence of the second concavity in the phase angle curves, suggests greater stability of the coatings to the action of the solution. Since the second concavity may be a result of electrolyte-metal interactions, non-porous, compact layers are expected in such cases. Consequently, a densification of the layer with increasing deposition power from 50 to 60 W is deduced from the phase angle and impedance analyses, in good agreement with the infrared results. The reduction in the film density when P is further increased (75 W) is suggested by the emergence of the second concavity in the curve corresponding to this sample. No detachment of the film was detected even after the electrochemical experiments.

The total resistance of the samples, R_t, which represents the sum of the electrolyte resistance, pore resistance and polarization resistance, evaluated from data of Fig. 9(a) and the model proposed by Mansfeld [39], is shown in Fig. 10(b) as a function of P for the pristine (dotted line) and coated stainless steel. Film deposition increases the total resistance of the substrate, independently of the deposition condition, but a rising trend is observed when P increases from 25 to 60 W; beyond this R_t stabilizes. An improvement of around 10,000 times in the total system resistance is detected for samples prepared at the highest powers (60 and 75 W). In addition to being superior to those obtained by acid passivation [40] the improvements obtained in the corrosion resistance of stainless steel shown here were produced by a dry, clean treatment, which does not create waste requiring special disposal.

The film thickness is a key parameter in the interpretation of such results. Considerable thickness variation (5 times) was detected when the excitation power was increased from 15 to 75 W (Fig. 1), but even the thinnest film (~400 nm) increased R_t by around 200 times. Fig. 11(a) shows the behavior of R_t as a function of the layer thickness, where an increase in R_t with increasing thickness is observed within particular P ranges (25–35 W and 50–60 W). For the other intervals, considerable variations in thickness did not promote changes in the total resistance. Moreover, changes in R_t are observed even at fixed film thickness (35 to 50 W), suggesting that it also depends on other variables.

Fig. 11(b) shows the effect of P on the R_t/h ratio, which provides the total resistance per unit of thickness (nm) of the material. R_t/h remains practically unchanged for samples prepared at low excitation powers (15–35 W), but continuously increases as P is elevated from 25 to 60 W, following exactly the same trend observed for [Si—O] and

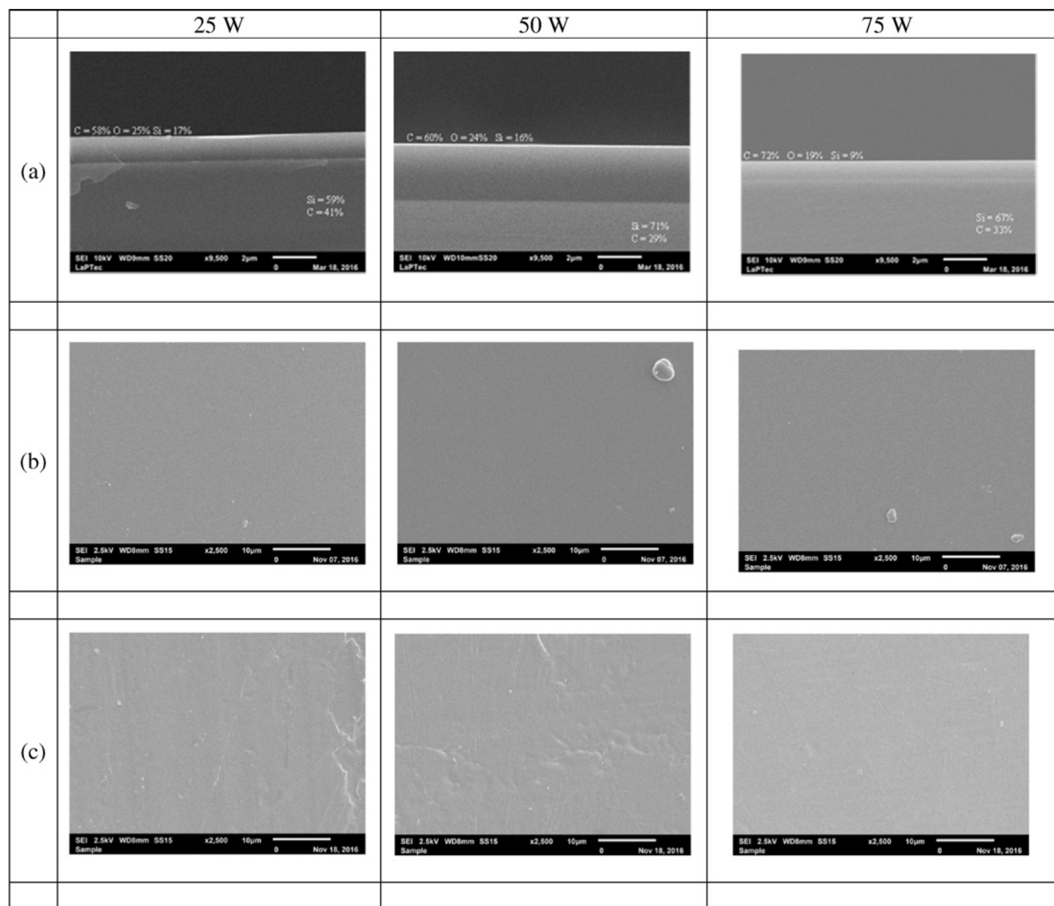

Fig. 7. (a) Cross-sectional and (b) top view secondary electrons micrographs of the samples deposited in plasmas of different powers on Si wafers. (c) Top view secondary electrons micrographs of the samples deposited in plasmas of different powers on stainless steel.

$[Si(CH_3)_x]$ derived from IR spectroscopy. That is, although there are changes in thickness, structural modifications play the major role in influencing R_t (Fig. 10(b)).

Fig. 12 shows the behavior of R_t as a function of the relative density of Si—O and $Si(CH_3)_x$ in the film structure. In both curves, if the point at 75 W is ignored, R_t tends to rise with increasing [SiO] and $[Si(CH_3)_x]$, revealing the major influence of the structure, more specifically of the densification, on the corrosion resistance. A substantial reduction in the relative density of Si—O and $Si(CH_3)_x$ groups was detected as P was increased from 60 to 75 W (Fig. 4(a) and (b)). According to the interpretation previously proposed, this reduction should promote a loss in corrosion protection, since it reflects structure rarefication, but this was not observed. It should be noted, however, that the thickness of the film deposited at 75 W was almost twice that of the film deposited at 60 W, which compensates for the structural modifications. Thus the thicknesses are responsible for the differences between these two samples, and can be used as an indicator for selecting the best deposition condition. The results of Figs. 11(a), (b) and 12 thus allow the distinction between the effects of thickness and structural variations on the total resistance of systems prepared here.

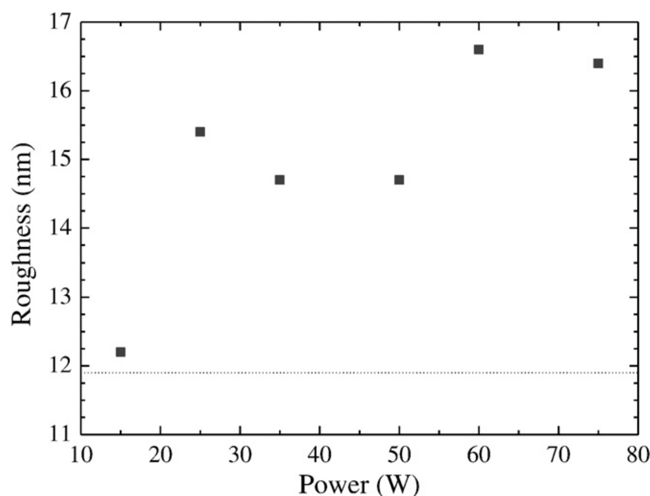

Fig. 8. Root mean square roughness of the films as a function of the plasma excitation power. The dotted line represents roughness of the bare substrate.

Owing to the structural and chemical similarities of the organosilicon HMDSO plasma-deposited films and the conventional PDMS polymer, their mechanical and tribological properties are similar to those of elastomers (depending on the degree of cross-linking). A prior investigation demonstrated that films deposited from HMDSO and O_2 plasma mixtures are highly resistant to scratching [41]. This characteristic, associated with transparency in the visible region, makes the organosilicon plasma deposited coatings attractive for protection of polymeric optical devices; moreover, these coatings are harder than conventional polymers and do not present the stress problems of silica layers deposited on flexible substrates [23]. Furthermore, Rangel et al. [42] have demonstrated that, despite their high carbon content, plasma-deposited organosilicon films are highly resistant to attack promoted by oxygen plasmas. This result is attributed to the formation of a silica layer upon exposition of the surface to reactive oxygen, thus protecting the organic underlayer. This explains why plasma polymerized HMDSO films present very good physical stability upon atmospheric aging [29]. All these characteristics are important regarding the

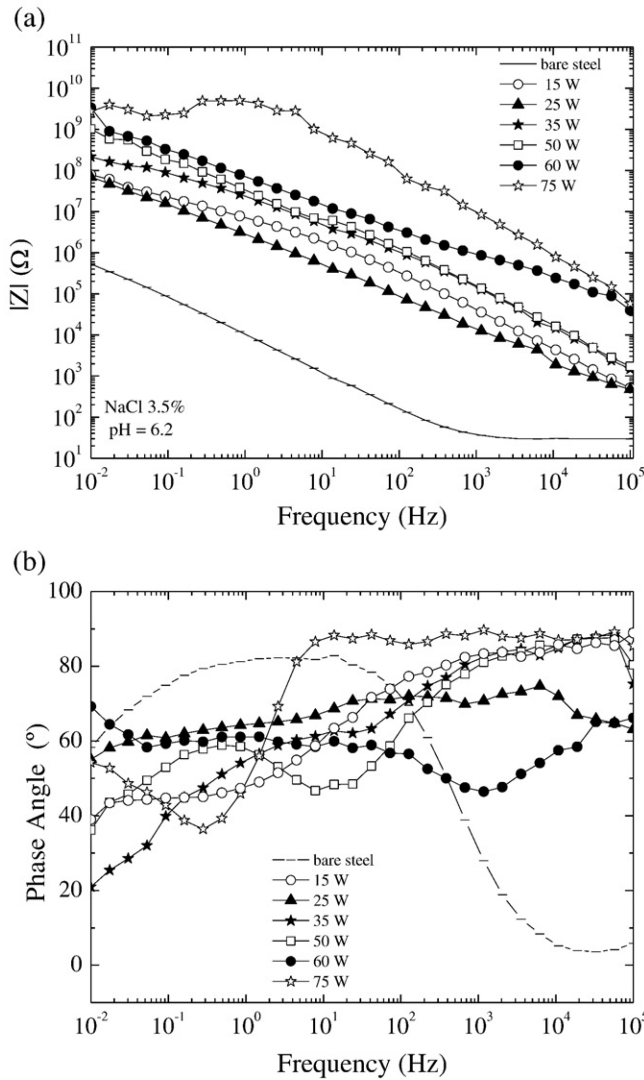

Fig. 9. (a) Impedance modulus as a function of frequency for the samples deposited at different excitation powers. The impedance modulus for the bare steel substrate is also presented. (b) Phase angle as a function of frequency for the samples deposited in plasmas of different powers. The phase angle for the bare steel substrate is also presented.

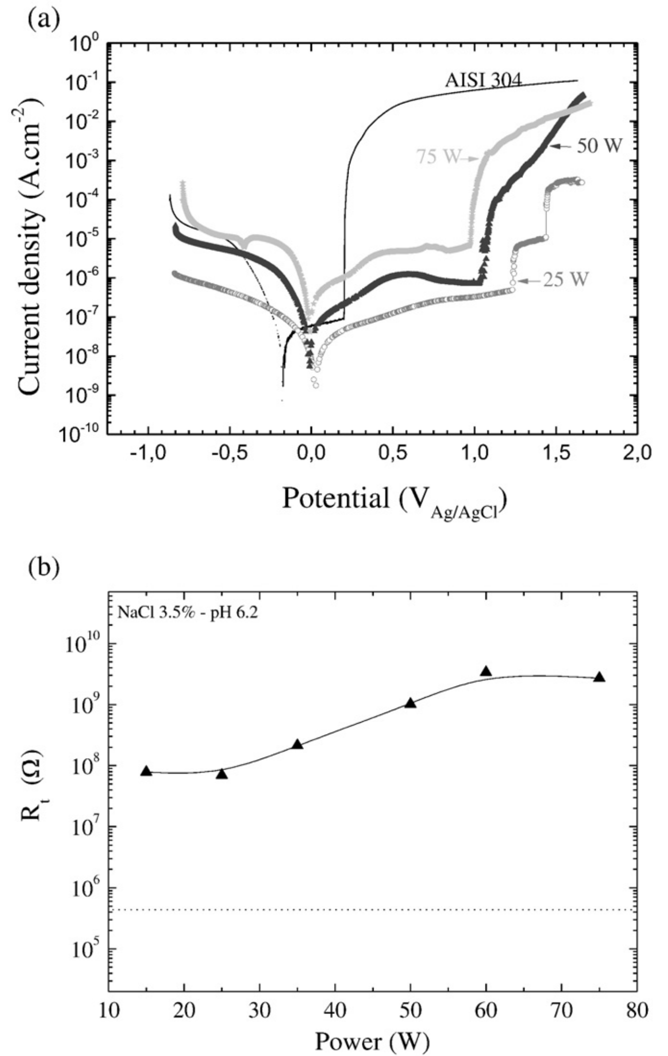

Fig. 10. (a) Potentiodynamic polarization curves and (b) total resistance of the systems coated with films of different thicknesses as a function of the plasma excitation power. The dotted line represents the total resistance for the untreated steel substrate.

durability of the coating applied as a corrosion barrier, and will be the subject of future investigations.

4. Conclusions

It was demonstrated that the plasma excitation power influences the properties of films deposited from HMDSO, oxygen and argon. A plasma polymer structure resembling conventional PDMS was obtained, with a degree of cross-linking dependent on the applied power.

Convenient changes in the chemical group structure, which contributed to the barrier properties of the coatings, were also observed. Deposition rate increased roughly fivefold with increasing plasma power. The greatest deposition rate was not optimal since it was detrimental to the barrier properties of the layer.

Despite the chemical structure modifications, chemical composition was barely affected. Indeed, the structural changes were sufficient to promote a crosslinked organosilicon structure highly resistant to saline solutions, the most hazardous environment for steels. Together with the degree of crosslinking, the proportion of silanol can be tailored by the plasma excitation power. No correlation was detected between corrosion resistance and roughness. The major parameters of interest were the film's structural resistance to saline solution, its impermeability to the electrolyte, and its physical stability even after electrochemical experiments.

Although the coatings prepared at 60 and 75 W presented different properties, they provided the same corrosion resistance for the metallic alloy. Considering the energy demands as well as the proportion of silanol groups, the coating prepared at 60 W is readily elected as optimal. This deposition condition, which improved the corrosion resistance of the stainless steel by four orders of magnitude, may also represent an excellent treatment for other less corrosion resistant metals.

A possible application for the layers prepared here is the construction of multilayered organosilicon/silica films, a better barrier system for protecting metallic substrates than single layers as both have the same thickness. To enable the construction of such devices the barrier

Table 2
Corrosion (E_{corr}) and pitting (E_{pit}) potentials for the as-received and coated stainless steel derived from potentiodynamic polarization tests.

Sample	E_{corr} (V)	E_{pit} (V)
Bare steel	−0.180	0.201
25 W	0.029	1.233
50 W	−0.001	1.028
75 W	−0.007	0.972

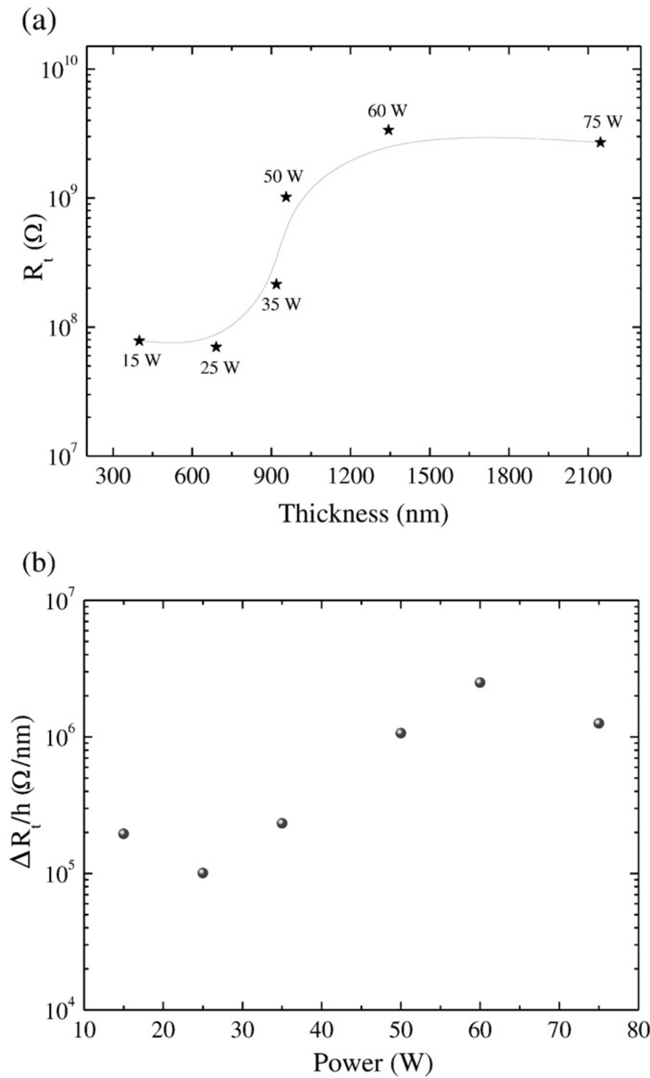

Fig. 11. (a) Total resistance of the systems as a function of the respective film thickness; (b) the total resistance variation per unit of thickness in the material as a function of the applied power.

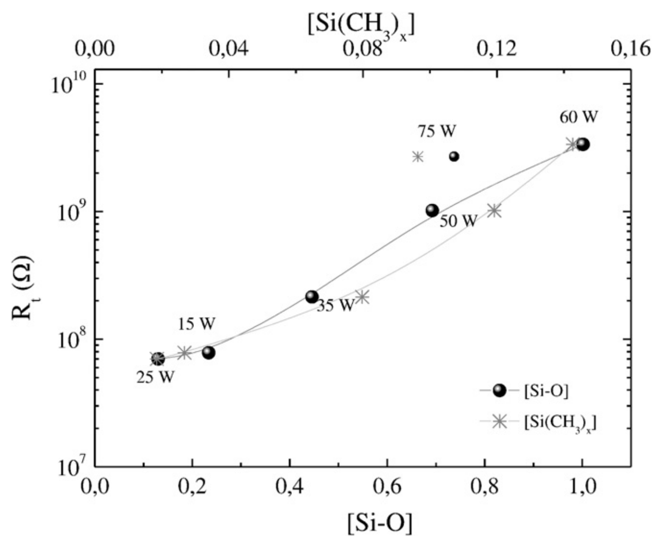

Fig. 12. Total resistance of the systems containing films with different thicknesses as a function of the relative density of SiO and $Si(CH_3)_x$.

properties as well as the optical, mechanical and tribological properties of films possessing the same thickness should be investigated.

Acknowledgements

The authors thank the Brazilian agencies FAPESP (2010/12240-8, 2012/14708-2 and 2014/21594-9) and CNPq (302446/2012-5, 301622/2012-4) for financial support.

References

[1] N. Alissawi, T. Peter, T. Strunskus, C. Ebbert, G. Grundmeier, F. Faupel, Plasma-polymerized HMDSO coatings to adjust the silver ion release properties of Ag/polymer nanocomposites, J. Nanopart. Res. 15 (2013) 2080–2092.

[2] L.F. Mobarakeh, R. Jafari, M. Farzaneh, The ice repellency of plasma polymerized hexamethyldisiloxane coating, Appl. Surf. Sci. 284 (2013) 459–463.

[3] N. Guermat, A. Bellel, S. Sahli, P. Raynaud, Electrical characterization and modeling of hexamethyldisiloxane thin film humidity sensors, J. Chem. Sci. Technol. 3 (2014) 13–17.

[4] H. Wang, L. Yang, Q. Chen, Investigation of microwave surface-wave plasma deposited SiO_x coatings on polymeric substrates, Plasma Sci. Technol. 16 (2014) 37–40.

[5] C.H. Tsai, Y.S. Li, I.C. Cheng, J.Z. Chen, O_2/HMDSO-plasma-deposited organic-inorganic hybrid film for gate dielectric of MgZnO thin-film transistor, Plasma Process. Polym. 11 (2014) 89–95.

[6] D.B.T. Mascagni, M.E.P. Souza, C.M.A. Freire, S.L. Silva, R.C.C. Rangel, N.C. Cruz, E.C. Rangel, Corrosion resistance of 2024 aluminum alloy coated with plasma deposited a-C:H:Si:O films, Mater. Res. 17 (2014) 1449–1465.

[7] Y.M. Ko, H.C. Choe, S.C. Jung, B.H. Kim, Plasma deposition of a silicone-like layer for the corrosion protection of magnesium, Prog. Org. Coat. 76 (2013) 1827–1832.

[8] C.J. Hall, P.J. Murphy, H.J. Griesser, Direct imaging of mechanical and chemical gradients across the thickness of graded organosilicone microwave PECVD coatings, ACS Appl. Mater. Interfaces 6 (2014) 1279–1287.

[9] M.F. Montemor, Functional and smart coatings for corrosion protection: a review of recent advances, Surf. Coat. Technol. 258 (2014) 17–37.

[10] T. Török, P. Urbán, G. Lassú, Surface cleaning and corrosion protection using plasma technology, Int. J. Corros. Scale Inhib. 4 (2015) 116–124.

[11] F. Khelifa, S. Ershov, M. Druart, Y. Habibi, D. Chicot, M. Olivier, R. Snyders, P. Dubois, A multilayer coating with optimized properties for corrosion protection of Al, J. Mater. Chem. A 3 (2015) 15977–15985.

[12] C. Vautrin-Ul, C. Boisse-Laporte, N. Benissad, A. Chausse, P. Leprince, R. Messina, Plasma-polymerized coatings using HMDSO precursor for iron protection, Prog. Org. Coat. 38 (2000) 9–15.

[13] C. Vautrin-Ul, F. Roux, C. Boisse-Laporte, J.L. Pastol, A. Chauss, Hexamethyldisiloxane (HMDSO)-plasma-polymerised coatings as primer for iron corrosion protection: influence of RF bias, J. Mater. Chem. 12 (2002) 2318–2324.

[14] M. Yekehtaz, K. Baba, R. Hatada, S. Flege, F. Sittner, W. Ensinger, Corrosion resistance of magnesium treated by hydrocarbon plasma immersion ion implantation, Nucl. Inst. Methods Phys. Res. B B267 (2009) 1666–1669.

[15] A.J. Choudhury, J. Chutia, H. Kakati, S.A. Barve, A.R. Pal, N.S. Sarma, D. Chowdhury, D.S. Patil, Studies of radiofrequency plasma deposition of hexamethyldisiloxane films and their thermal stability and corrosion resistance behavior, Vacuum 84 (2010) 1327–1333.

[16] N.D. Boscher, P. Choquet, D. Duday, S. Verdier, Chemical compositions of organosilicon thin films deposited on aluminum foil by atmospheric pressure dielectric barrier discharge and their electrochemical behaviour, Surf. Coat. Technol. 205 (2010) 2438–2448.

[17] J. Schwartz, M. Schmidt, Synthesis of plasma-polymerized hexamethyl disiloxane (HMDSO) films by microwave discharge, Surf. Coat. Technol. 98 (1998) 859–864.

[18] F. Fanelli, F.R. d'Agostino, F. Fracassi, GC–MS investigation of hexamethyldisiloxane-oxygen fed cold plasmas: low pressure versus atmospheric pressure operation, Plasma Process. Polym. 8 (2011) 932–941.

[19] E. Vassallo, A. Cremona, L. Laguardia, E. Mesto, Preparation of plasma-polymerized SiO_x-like thin films from a mixture of hexamethyldisiloxane and oxygen to improve the corrosion behaviour, Surf. Coat. Technol. 200 (2006) 3035–3040.

[20] C. Petit-Etienne, M. Tatoulian, I. Mabille, E. Sutter, F. Arefi-Khonsari, Deposition of SiO_x-like thin films from a mixture of HMDSO and oxygen by low pressure and DBD discharges to improve the corrosion behaviour of steel, Plasma Process. Polym. 4 (2007) S562–S567.

[21] L. Zhou, G.L.V.H. Pang, G. Zhang, S. Yang, Comparing deposition of organic and inorganic siloxane films by atmospheric pressure glow discharge, Surf. Coat. Technol. 206 (2012) 2552–2557.

[22] M.R. Alexander, F.R. Jones, R.D. Short, Radio-frequency hexamethyldisiloxane plasma deposition: a comparison of plasma- and deposit-chemistry, Plasmas Polym. 2 (1997) 277–300.

[23] L. Zajíčková, V. Buršíková, Z. Kučerová, D. Franta, P. Dvořák, R. Šmíd, V. Peřina, A. Macková, Deposition of protective coatings in rf organosilicon discharges, Plasma Sources Sci. Technol. 16 (2007) S123–S132.

[24] R.C.C. Rangel, T.C. Pompeu, J.L.S. Barros Jr., C.A. Antonio, N.M. Santos, B.O. Pelici, C.M.A. Freire, N.C. Cruz, E.C. Rangel, Improvement of the corrosion resistance of carbon steel by plasma deposited thin films, in: R.S. Razavi (Ed.), Recent Researches in Corrosion Evaluation and Protection, Intech, Rijeka 2012, pp. 91–116.

[25] S.D. Mancini, A.R. Nogueira, E.C. Rangel, N.C. Cruz, Solid-state hydrolysis of postconsumer polyethylene terephthalate after plasma treatment, J. Appl. Polym. Sci. 127 (2013) 1989–1996.
[26] F. Fracassi, R. d'Agostino, F. Palumbo, E. Angelini, S. Grassini, F. Rosalbino, Application of plasma deposited organosilicon thin films for the corrosion protection of metals, Surf. Coat. Technol. 174–175 (2003) 107–111.
[27] Y. Zhou, D. Probst, A. Thissen, E. Kroke, R. Riedel, R. Hauser, H. Hoche, E. Broszeit, P. Kroll, H. Stafast, Hard silicon carbonitride films obtained by RF-plasma-enhanced chemical vapour deposition using the single-source precursor bis(trimethylsilyl)carbodiimide, J. Eur. Ceram. Soc. 26 (2006) 1325–1335.
[28] M.D.F. Albuquerque, E. Santos Jr., R.R.T. Perdone, R.A. Simão, Effect of self-bias voltage on the wettability, chemical functionality and nanomechanical properties of hexamethyldisiloxane films, Thin Solid Films 564 (2014) 73–78.
[29] T.R. Gengenbach, H.J. Griesser, Post-deposition ageing reactions differ markedly between plasma polymers deposited from siloxane and silazane monomers, Polymer 40 (1999) 5079–5094.
[30] S. Kurosawa, B.G. Choi, J.W. Park, H. Aizawa, K.B. Shim, K. Yamamoto, Synthesis and characterization of plasma-polymerized hexamethyldisiloxane films, Thin Solid Films 506-507 (2006) 176–179.
[31] N.E. Blanchard, B. Hanselmann, J. Drosten, M. Heuberger, D. Hegemann, Densification and hydration of HMDSO plasma polymers, Plasma Process. Polym. 12 (2015) 32–41.
[32] W.A. Lanford, M.J. Rand, The hydrogen content of plasma-deposited silicon nitride, J. Appl. Phys. 49 (1978) 2473–2477.
[33] M.R. Alexander, R.D. Short, F.R. Jones, W. Michaeli, C.J. Blomfield, Appl. Surf. Sci. 137 (1999) 179–183.
[34] L.A. O'Hare, A. Hynes, M.R. Alexander, Surf. Interface Anal. 39 (2007) 926–936.
[35] N.D. Boscher, P. Choquet, D. Duday, S. Verdier, Plasma Process. Polym. 7 (2010) 163–171.
[36] A.J. Choudhury, M.R. Alexander, F.R. Jones, R.D. Short, Plasmas Polym. 2 (1997) 4.
[37] Y. Wang, J. Zhang, X. Shen, Surface structures tailoring of hexamethyldisiloxane films by pulse rf plasma polymerization, Mater. Chem. Phys. 96 (2006) 498–505.
[38] M. Ricci, J. Dorier, C. Hollenstein, P. Fayet, Influence of argon and nitrogen admixture in HMDSO/O_2 plasmas onto powder formation, Plasma Process. Polym. 8 (2011) 108–117.
[39] F. Mansfeld, Recording and analysis of AC impedance data for corrosion studies, Corrosion 37 (1981) 301–307.
[40] J.J. Kim, Y.M. Young, Study on the passive film of type 316 stainless steel, Int. J. Electrochem. Sci. 8 (2013) 11847–11859.
[41] B.B. Lopes, R.C.C. Rangel, C.A. Antonio, S.F. Durrant, N.C. Cruz, E.C. Rangel, Mechanical and tribological properties of plasma deposited a-C:H:Si:O films, in: J. Nemecek (Ed.), Nanoindentation in Materials Science, Intech, Rijeka 2012, pp. 179–201.
[42] R.C.C. Rangel, T.C. Pompeu, J.L.S. Barros Jr., C.A. Antonio, N.M. Santos, B.O. Pelici, C.M.A. Freire, N.C. da Cruz, E.C. Rangel, Improvement of the corrosion resistance of carbon steel by plasma deposited thin films, Recent Researches in Corrosion Evaluation and Protection, Reza Shoja Razavi, Intech Open Access Publisher 2012, pp. 91–116 (Retrieved from http://www.intechopen.com/articles/show/title/improvement-of-the-corrosion-resistance-of-carbon-steel-by-plasma-deposited-thin-films).